

Crossing angle at the photon collider

V.I. Telnov

Institute of Nuclear Physics, 630090 Novosibirsk, Russia

For removal of disrupted beams at the ILC linear e^+e^- collider it is desirable to collide beams at some crossing angle. An especially large crossing angle, of about 25 mrad, is necessary for the photon collider, where disrupted beams are softer and wider than in the e^+e^- case. Some complications arise due to the solenoidal magnetic field of the detector. Radiation of particles in this field can increase the vertical beam size, leading to a loss of the luminosity. In addition, in the presence of a detector magnetic field the beam trajectories are not flat. Moreover, in the case of e^-e^- beams, the vertical collision angle is non-zero and larger than the beam diagonal angle σ_y/σ_z , and this should be corrected in some way. In this paper, possible solutions of these problems are considered. It is shown that at the ILC one can have the interaction region compatible both with e^+e^- and $\gamma\gamma$, γe modes of operation without loss of luminosity.

1. INTRODUCTION

At photon colliders, high energy photon beams are produced by Compton scattering of laser photons off high energy electrons in linear colliders [1, 2]. Due to multiple Compton scattering the beams after the $e \rightarrow \gamma$ conversion have a large energy spread: $E = (0.02-1)E_0$ [3, 4, 5, 6]. After the collision with the opposing electron beam, low energy electrons acquire disruption angles $\theta_d \sim 10-12$ mrad (background from particles with larger angles is less than that from other unavoidable backgrounds) [6]. Large energy and angular spreads of the beams present a problem of the removal of beams from the detector.

The crab-crossing scheme of the beam collisions at e^+e^- linear colliders [7] presents a very nice solution to the above problems at the photon collider [3], Fig. 1. Though the collision angle α_c is larger than the horizontal diagonal angle of the beam at the interaction point (IP), σ_x/σ_z , there is no loss of the luminosity because each beam is tilted using a special RF cavity) by the angle $\alpha_c/2$. Due to this collision angle, the outgoing disrupted beams travel outside the final quads. The value of the crab-crossing angle is determined by the disruption angles and by the final quad

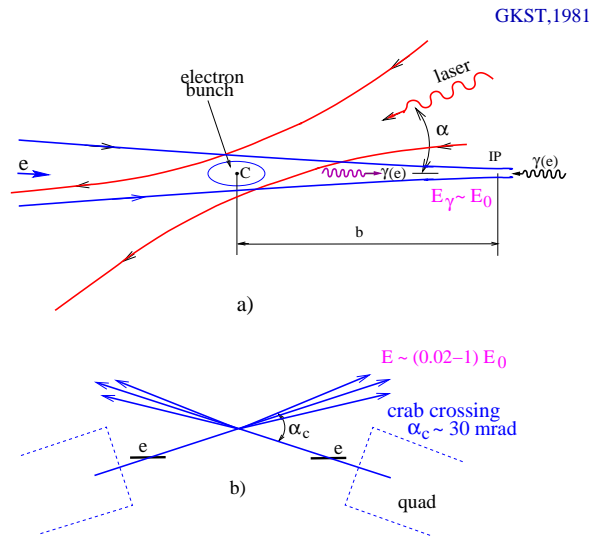


Figure 1: Scheme of the beam collisions at the photon collider

design (the diameter of the quad and its distance from the IP):

$$\alpha_c \sim R_{quad}/L^* + \theta_d \sim 6 \text{ cm} / 400 \text{ cm} + 0.01 \sim 25 \text{ mrad}. \quad (1)$$

For e^+e^- collisions, $\alpha_c = 20 \text{ mrad}$ is one of the considered options. It is very desirable to have the crossing compatible with both collision modes, i.e. $\alpha_c \sim 20\text{--}25 \text{ mrad}$.

There are several problem associated with a large crab-crossing angle:

- stability of the beam tilt (provided by the crab-cavity) with an accuracy better than $(\sigma_x/\sigma_z)/\alpha_c \sim 10^{-2}$;
- the increase of the vertical beam size due to radiation in the detector fields must be much smaller than the vertical beam size determined by the beam emittance;
- the non-zero vertical collision angle at the IP due to the detector field should be corrected;
- the dilution of the horizontal beam emittance due to the bend (needed for obtaining of the required crossing angle) should be small, and the bending length should be reasonable.

Below we consider the three last items (the first one is a separate technical task) and find the maximum value of α_c for the considered detectors that satisfies all the above criteria.

2. THE ANGLE BETWEEN TUNNELS, THE BENDING ANGLE

Possible configurations of the ILC tunnels with two IPs are shown in Fig. 2. The increase of the normalized

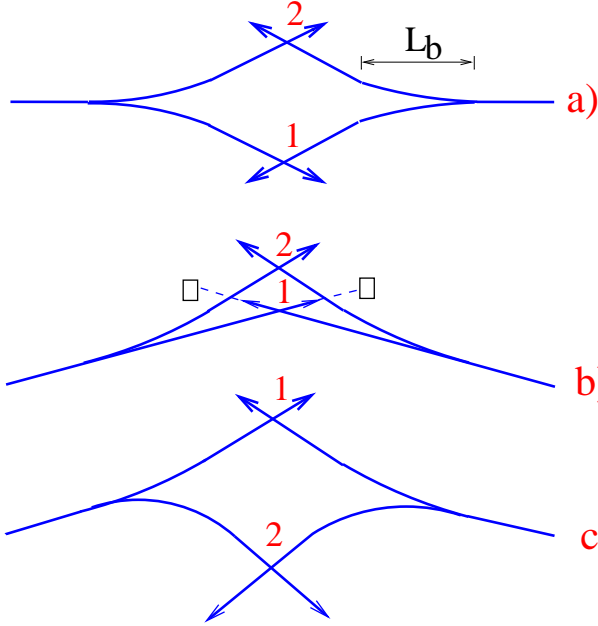


Figure 2: Possible configurations of tunnels at the ILC. The crab-crossing angle for e^+e^- (IP1) is about $\alpha_{c,1} = 0\text{--}20 \text{ mrad}$, smaller than that for $\gamma\gamma$ (IP2), which is $\alpha_{c,2} \sim 25 \text{ mrad}$.

Scheme a: the angle between the tunnels is zero. This is the simplest configuration, the only problem: for maximum beam energies the bending length L_b required for a small emittance dilution may be too long.

Scheme b: the angle between tunnels is non-zero, bending angles are minimum, but there may be problems with the space for detectors and for dumping of beams at IP1.

Scheme c: the angle between tunnels is non-zero, as in the scheme a) the beams are bent in opposing directions, there is no problem with the space, but due to different bending angles the maximum energies for IP1 and IP2 are different. This scheme has sense only when tunnels will be used in future for other multi-TeV linear collider.

horizontal beam emittance due to synchrotron radiation (SR) after the bending by the angle α_b [11, 12] is

$$\Delta\epsilon_{nx} \propto \frac{E^6 \alpha_b^5}{L_b^4}. \quad (2)$$

Taking the coefficient from the NLC ZDR [8], one gets

$$\Delta\epsilon_{nx} = 1.8 \times 10^{-10} \left(\frac{2E_0}{\text{TeV}} \right)^6 \left(\frac{\text{km}}{L_b} \right)^4 \left(\frac{\alpha_b}{10 \text{ mrad}} \right)^5 \text{ m}. \quad (3)$$

Table I: The length required for the bending on the angle 10 mrad for several beam energies

$2E_0$ TeV	1	2	3	5
L_b km	0.2	0.57	1.04	2.25

The bending length corresponding to a 5% emittance dilution at $\epsilon_{nx} = 2 \times 10^{-6}$ m and $\alpha_b = 10$ mrad is given in Table I for several beam energies.

The choice of scheme depends on the assumed maximum energy of the collider in these tunnels. For the ILC with $2E_0 = 1$ TeV, the required bending length is quite small and one can use a zero angle between tunnels (scheme a)). For multi-TeV colliders the schemes b) and c) are preferable, but in the latter case only one IP can work at the highest energy.

3. MOTION OF PARTICLES IN THE DETECTOR FIELDS

The longitudinal magnetic field in the detector, $B(z)$, is maximum at the center and decreases to zero at $z \rightarrow \infty$. From conservation of the flux we can find the radial field (fringe field) at the coordinate z on the beam trajectory:

$$B_r = -\frac{\partial B_z}{\partial z} \frac{r}{2} = -\frac{\partial B_z}{\partial z} \frac{\theta_0 z}{2}, \quad (4)$$

where $\theta_0 = \alpha_c/2$.

The total force acting on the electron in the vertical direction is

$$F_y = e \frac{v}{c} (-B_z \theta_0 + B_r) = -e \frac{v}{c} \theta_0 \left(B_z + \frac{\partial B_z}{\partial z} \frac{z}{2} \right). \quad (5)$$

The vertical coordinate at the position z for a particle traveling from the infinity is

$$y = \int_z^\infty (z' - z) y''(z') dz', \quad (6)$$

where $y'' \equiv d^2 y / dz^2 \approx F_y / P v$. Substituting (4,5) to (6) and integrating by parts, we can calculate the vertical coordinate at $z = 0$:

$$y(0) = \frac{e \theta_0}{P c} \left(\int_0^\infty B_z z dz + \int_0^\infty \frac{z^2}{2} dB_z \right) = \frac{e \theta_0}{P} \left(\int_0^\infty B_z z dz + B_z \frac{z^2}{2} \Big|_0^\infty - \int_0^\infty B_z z dz \right) = 0. \quad (7)$$

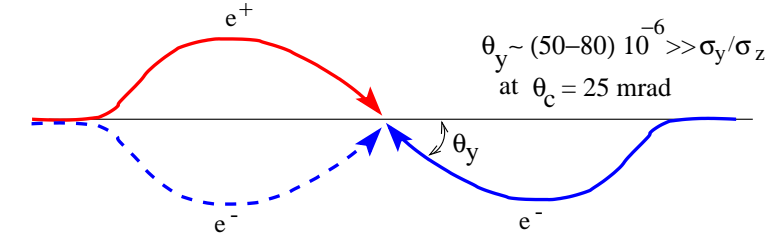
This interesting result was obtained in ref.[9] in a more complicated way.

The vertical collision angle at the IP is given by

$$\theta_y(z=0) = \frac{e \theta_0}{P c} \left(\int_0^\infty B_z dz + \int_0^\infty \frac{z}{2} dB_z \right) = \frac{e \theta_0}{P c} \left(\int_0^\infty B_z dz + B_z \frac{z}{2} \Big|_0^\infty - \int_0^\infty \frac{B_z}{2} dz \right) = \frac{e \theta_0}{2 P c} \int_0^\infty B_z dz. \quad (8)$$

We see that the radial fringe field reduces the angle at the IP by a factor of 2 compared to the action of the longitudinal magnetic field. This is a new result.

It is important to note that in the e^+e^- case each beam has a vertical angle at the IP with respect to the horizontal plane but their angle with respect to one another is zero: the beams collide head-on. On the contrary, in the e^-e^- case beams collide at the angle $2\theta_y$, see Fig. 3 (upper). This situation is acceptable for e^+e^- collisions. Beams collide head-on, and the tilt of the collision line is rather small. For example, the vertical displacement of beamstrahlung photons at the entrance to the first quadrupole at the distance 4 m from the IP will only be about 200–300 μm . The additional spin-precession angle due to the tilt of the collision line is of the order of 1° , which is negligible and can be corrected by the spin rotator at the entrance to the linac.



OK for e^+e^- , but not OK for $e^-e^- (\gamma\gamma)$

A vertical shift of the final quadrupoles helps
for $e^-e^- (\gamma\gamma)$

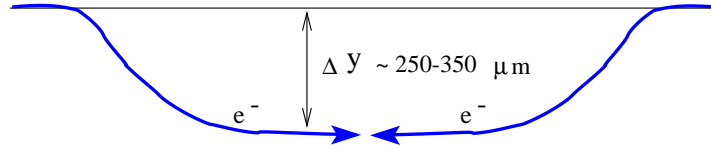


Figure 3: Trajectories of e^+e^- and e^-e^- beams

For e^-e^- collisions, the diagonal angle $\sigma_y/\sigma_z \sim 5 \times 10^{-7} \text{ cm} / 3 \times 10^{-2} \text{ cm} \sim 1.5 \times 10^{-5}$ is smaller than the relative collision angle $2\theta_y$ by a factor of ten, which means a considerable loss of luminosity. The situation can be corrected by shift of the first quadrupoles (they will act as dipole magnets), resulting in the beams colliding in the horizontal plane, see Fig. 3 (lower). The vertical displacement of the IP of 250-350 μm does not make any problems.

In addition to above method of the correction there is a suggestion to use additional coils in the detector (Detector Integrated Dipole), which allows to correct not only the collision angle but the vertical position at the IP [10]. I do not think that these complications are necessary. Moreover, in this case the detector loses its azimuthal symmetry.

4. GROWTH OF THE VERTICAL BEAM SIZE DUE TO SYNCHROTRON RADIATION

The large crab-crossing angle leads to the increase of σ_y due to synchrotron radiation of particles in the detector field. After emission of the photon(s) the electron comes to the IP with some vertical deflection. This effect leads to the decrease of the luminosity. The additional vertical r.m.s. spread is [8, 13]

$$\sigma_{y,SR}^2 = \frac{55r_e^2}{480\sqrt{3}\alpha} \left(\frac{eB_s\alpha_c L}{2mc^2} \right)^5. \quad (9)$$

The number of photons emitted by the electron in the transverse magnetic field B on the length L is [14]

$$N_\gamma = \frac{5\alpha eBL}{2\sqrt{3}mc^2} \sim 0.01\gamma\theta_b = 0.005 \frac{eB_s\alpha_c L}{mc^2}, \quad (10)$$

where $\alpha \approx 1/137$ and $\theta_b = eBL/E_0$ is the bending angle. For example, $B_s = 4 \text{ T}$, $\alpha_c = 30 \text{ mrad}$, $L = 4 \text{ m} \Rightarrow N_\gamma \sim 1.4$. So, the number of SR photons/electron $N_\gamma \propto LB_s\alpha_c = \mathcal{O}(1)$, which means that the distribution of y is non-Gaussian and so one cannot use Eq. 9. In addition, the fields in detectors are nonuniform. All this can be accounted for only by simulation.

The simulation was done using PHOCOL code [4, 6], which simulates beam collisions at linear colliders in all modes. It was used for simulation of photon colliders for NLC ZDR, TESLA CDR, TESLA TDR. The effect of SR was taken into account in the following way. Using the map of the magnetic field in the detector (as we saw, $B(z, 0, 0)$ is sufficient), the emission of SR photons was simulated and the deviation of the electron position at the IP

from the case when there is no SR was calculated for each electron. This deviation was added to the initial Gaussian position of the electron at $z = 0$. Then all particles were shifted according to their coordinates and angles at the IP to their starting positions at $z > 5\sigma_z$ (or CP-IP distance at the photon collider) and the simulation with account of all collision effects was started. In the given simulation (e^+e^- at $2E_0=1$ TeV) only attraction between particles was switched on (other processes are not essential).

Beam parameters were taken from U.S. Linear Collider Technology Option Study: $2E_0 = 1$ TeV, $N = 2 \times 10^{10}$, $\sigma_z = 0.3$ mm, $\epsilon_{nx}=9.6 \times 10^{-6}$ m, $\epsilon_{ny}=0.04 \times 10^{-6}$ m, $\beta_x = 24.4$ mm, $\beta_y = 0.4$ mm, $\sigma_x = 490$ nm, $\sigma_y = 4$ nm.

For the $\gamma\gamma$ case, instead of the $\gamma\gamma$ luminosity I simulated the e^-e^- luminosity (without the $e \rightarrow \gamma$ conversion) with $\sigma_y(\gamma\gamma) = \sqrt{2}\sigma_y(e^+e^-)$ in order to take into account an effective increase of the vertical beam size due to the Compton scattering. All interactions between particles were switched off. The position of the first quad (shifted in the $e^-e^-(\gamma\gamma)$ case in order to have a zero collision angle) was $z = 3.5\text{--}5.7$ m for all detectors.

The detector fields $B(z, 0, 0)$ in the LD(TESLA) [16], SID [15] and GLD [17] detectors used for simulation are presented in Fig. 4.

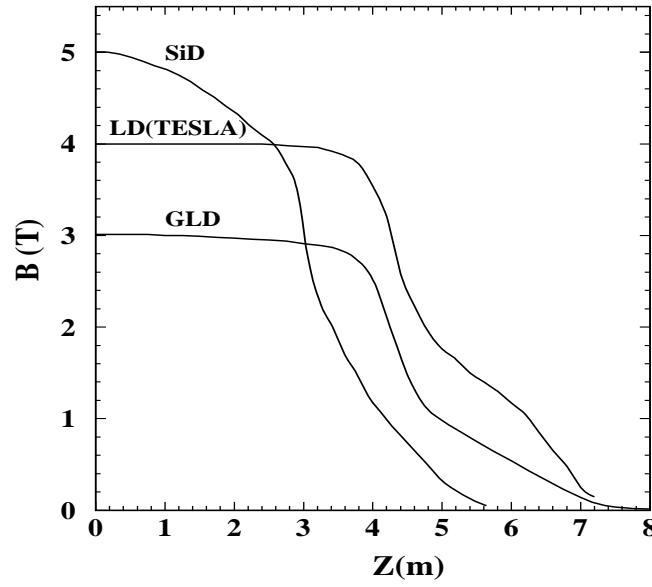


Figure 4: T $B(z, 0, 0)$ in LD, SID and GLD detectors

Results of the simulation are presented in Table 4, the statistical accuracy is about $\pm 0.5\%$. We see that the

Table II: Results on $L(\alpha_c)/L(0)$.

e^+e^- collisions

$\alpha_c(\text{mrad})$	0	20	25	30	35	40
LD(TESLA)	1.	0.98	0.95	0.88	0.83	0.76
SID	1.	0.995	0.985	0.98	0.95	0.91
GLD	1.	0.995	0.98	0.97	0.94	0.925

$\gamma\gamma$ collisions

$\alpha_c(\text{mrad})$	0	20	25	30	35	40
LD(TESLA)	1	0.99	0.96	0.925	0.86	0.79
SID	1	0.99	0.975	0.955	0.91	0.86
GLD	1	0.995	0.985	0.98	0.97	0.93

crab-crossing angle $\alpha_c = 25$ mrad is acceptable for all detectors in the e^+e^- and $\gamma\gamma$ modes of operation. For $\alpha_c = 30$ mrad, the luminosity loss with the LD(TECLA) detector is already about 12%, but possibly it can be decreased by proper shaping of the magnetic field.

5. CONCLUSION

One of the interaction regions at the linear collider intended for e^+e^- and then for $\gamma\gamma$ collisions should have a crab-crossing angle about 25 mrad. In this paper I considered problems caused by such a large crossing angle. The vertical collision angle between electron beams due to the detector magnetic field can be corrected by shifting the first quadrupoles. It is shown that the decrease of the e^+e^- and $\gamma\gamma$ luminosities due to synchrotron radiation is small up to the crab-crossing angle $\alpha_c = 25$ mrad. So, one can have the interaction region at the ILC compatible with both e^+e^- and $\gamma\gamma$ modes of operation.

Acknowledgments

I would like to thank A. Seryi for useful discussions.

References

- [1] I.F. Ginzburg, G.L. Kotkin, V.G. Serbo, V.I. Telnov, *Pizma ZhETF*, **34** (1981) 514; *JETP Lett.* **34** (1982) 491.
- [2] I.F. Ginzburg, G.L. Kotkin, V.G. Serbo, V.I. Telnov, *Nucl. Instr. & Meth.* **205** (1983) 47.
- [3] V. I. Telnov. *Nucl. Instr. & Meth.*, **A294** (1990) 72.
- [4] V.I. Telnov, *Nucl. Instr. & Meth.* **355** (1995) 3.
- [5] R. Brinkmann et al, *Nucl. Instr. & Meth.* **A406** (1998) 13.
- [6] B. Badelek et. al., *Intern. Journ. Mod. Phys. A* **30** (2004) 5097-5186.
- [7] R.B. Palmer, SLAC-PUB-4707.
- [8] J. Irwin, in *Zeroth-Order Design Report for the NLC*, LBNL-5424, SLAC-474, 1996.
- [9] P. Tenenbaum, J. Irwin and T. O. Raubenheimer, *Phys. Rev. ST Accel. Beams* **6**, 061001 (2003).
- [10] B. Parker and A. Seryi, SLAC-PUB-11038.
- [11] R. H. Helm, M. J. Lee, P. L. Morton and M. Sands, *IEEE Trans. Nucl. Sci.* **20** (1973) 900.
- [12] T. O. Raubenheimer, P. Emma and S. Kheifets, SLAC-PUB-6119.
- [13] V. I. Telnov, *Proc. of the Summer Study on the Future of Particle Physics (Snowmass 2001)* ed. N. Graf, eConf **C010630**, T104 (2001).
- [14] J.D. Jackson, *Classical Electrodynamics*, 2nd edition (John Wiley and Sons, New York, 1975).
- [15] Y. Nosochkov and A. Seryi, *Phys. Rev. ST Accel. Beams* **8**, 021001 (2005).
- [16] G. Bernard, private communication.
- [17] H. Yamaoka, private communication.